Chaos and its quantization in dynamical Jahn-Teller systems

Hisatsugu Yamasaki* and Yuhei Natsume
Graduate School of Science and Technology, Chiba-University, Inage-ku, Chiba 263-8522, Japan

Akira Terai and Katsuhiro Nakamura
Department of Applied Physics, Osaka City University, Sumiyoshi-ku, Osaka 558-8585, Japan

(Received 21 April 2003; revised manuscript received 18 July 2003; published 2 October 2003)

We investigate the $E_g \otimes e_g$ Jahn-Teller system for the purpose of revealing the nature of quantum chaos in crystals. This system simulates the interaction between the nuclear vibrational modes and the electronic motion in non-Kramers doublets for multiplets of transition-metal ions. Inclusion of the anharmonic potential due to the trigonal symmetry in crystals makes the system nonintegrable and chaotic. Besides the quantal analysis of the transition from Poisson to Wigner level statistics with increasing the strength of anharmonicity, we study the effect of chaos on the electronic orbital angular momentum and explore the magnetic *g*-factor as a function of the system's energy. The regular oscillation of this factor changes to a rapidly decaying irregular oscillation by increasing the anharmonicity (chaoticity).

DOI: 10.1103/PhysRevE.68.046201 PACS number(s): 05.45.Mt, 31.30.Gs, 71.70.Ej, 82.90.+j

I. INTRODUCTION

Recently the study on quantization of classically chaotic Hamiltonian systems has received wide attention. An accumulation of numerical and experimental data indicates Wigner-type level statistics, wave function scars, and other characteristic features [1,2].

In addition to toy models such as a kicked rotator, Hénon-Heiles system, some realistic systems such as a hydrogen atom in a magnetic field and microwave cavities are also being investigated [1–3]. Quantum mechanics of chaotic systems also suggests insight beyond a simple quantal manifestation of chaos [4,5]. Therefore, it is crucial to have more and more experimentally accessible quantum systems which exhibit chaos in its classical treatment.

In this paper we choose the Jahn-Teller system simulating transition-metal ions embedded in the host crystals such as III-V semiconductors and halides crystals. Among them we consider the $E_g \otimes e_g$ model associated with the irreducible representation for the cubic symmetry group, namely, the two-dimensional (2D) lattice-vibration modes e_g linearly coupled to doubly degenerate electronic states E_g [6]. This system has an adiabatic doubly folded lattice potential with the conical intersection of the potential surfaces, whose geometric phase was one of the topics some time ago [7,8]. The lattice potential here can be harmonic or anharmonic. From the classical dynamical viewpoint in the adiabatic limit, as shown below, the system with the 2D harmonic potential is integrable, leading to regular motions, and on adding the anharmonic term, it becomes nonintegrable and chaotic [9]. A systematic investigation of the quantal counterpart of classical chaos in these systems is desirable. Furthermore, since the model is a representative for paramagnetic ions, it is experimentally important to see the effect of chaos on the magnetic g factor. This factor is an expectation value for electronic orbital angular momentum and measures a degree of level splitting of highly excited states induced by the lattice-electron interaction. The oscillating structure in the energy dependence of the g factor is expected to reflect the feature of the underlying classical dynamics.

The organization of the paper is as follows. In Sec. II a model for Jahn-Teller $E_g \otimes e_g$ system is proposed. Section III deals with the classical analyses of the model. Both the systems, with and without anharmonic terms, are examined. Section IV presents a quantization of the system together with the level statistics. Section V is concerned with a proposal of the experiment to verify the quantum signature of chaos in the dynamical Jahn-Teller system. A novel effect on the g factor is explored there. Final section is devoted to summary and discussions.

II. DYNAMICAL JAHN-TELLER SYSTEM

We investigate the electronic states of degenerate E_g orbitals of d levels in transition-metal ions coupled with 2D vibrational modes e_g expressed by coordinates Q_1 and Q_2. The $E_g \otimes e_g$ model is the typical system showing dynamic Jahn-Teller effects, which has been discussed in the field of magnetism for transition-metal ions [6,10]. The Hamiltonian matrix H for this system is expressed as

$$H = -\frac{\hbar^2}{2}\left(\frac{\partial^2}{\partial Q_1^2} + \frac{\partial^2}{\partial Q_2^2}\right)\mathbf{I} + k\begin{bmatrix} Q_1 & Q_2 \\ Q_2 & -Q_1 \end{bmatrix} + V(\mathbf{Q})\mathbf{I}, \quad (1)$$

where $\mathbf{I}$ is the 2×2 unit matrix and $V(\mathbf{Q})$ is a potential energy. The nuclear mass is set to unity. The second term of Eq. (1) is the so-called Jahn-Teller interaction H_{J-T} with k being the coupling parameter between electronic states and vibrational modes. Bases for electronic orbitals E_g lying behind Eq. (1) are $\langle \mathbf{r}|u\rangle = u(\mathbf{r}) = 3z^2 - r^2$ and $\langle \mathbf{r}|v\rangle = v(\mathbf{r}) = x^2 - y^2$. When $V(\mathbf{Q})$ is a harmonic potential given by

$$V_0(\mathbf{Q}) = \frac{1}{2}\omega^2(Q_1^2 + Q_2^2), \quad (2)$$

*Electronic address: hisa@physics.s.chiba-u.ac.jp;
URL: http://zeong.s.chiba-u.ac.jp/~hisa/

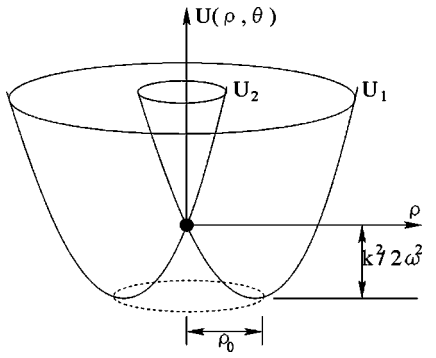

FIG. 1. Adiabatic potential of Mexican-hat or sombrero shape. $\rho=\sqrt{Q_1^2+Q_2^2}$. The potential has the degenerate minimum.

the corresponding adiabatic potential for Eq. (1) has the Mexican-hat or sombrero shape in Fig. 1, where $Q_1=\rho\cos\theta$ and $Q_2=\rho\sin\theta$. The potential minima lie at $\rho=\rho_0=k/\omega^2$ with an arbitrary value of θ. Namely, the minima are infinitely degenerate. The energy for the minima is $k^2/2\omega^2$. Vibronic levels for the quantum Hamiltonian (1) were discussed in numerical calculations using small dimensional Hamiltonian matrices [11]. Recently this model has been investigated from a viewpoint of the geometric phase [10,12]. On the other hand, the effect of the trigonal fields expressed as the anharmonic term,

$$V_A(\mathbf{Q})=-(b/3)(Q_1^3-3Q_1Q_2^2), \tag{3}$$

was also analyzed as to some low-lying levels [11,13]. In short, O'Brien investigated system (1) with potential $V(\mathbf{Q})=V_0(\mathbf{Q})+V_A(\mathbf{Q})$ in the low-energy approximation that ρ is fixed to ρ_0. However, we numerically calculate eigenvalues and eigenvectors without having recourse to such an approximation. We derive level-spacing distributions to see the effect of chaos on quantum systems [1–3,14–16]. Furthermore we investigate the quantal g factor, whose oscillating structure was shown three decades ago by Washimiya in the system without anharmonicity. We explore the effect of chaos on the g factor in the system with the anharmonicity. The dynamical Jahn-Teller (JT) system was also studied by Bulgac and Kusnezov [17–20] in a system with the three-dimensional harmonic potential. However, we should note that the dimensionality of lattice-vibration modes characterized by the irreducible representation is two and not three according to the theory of a point-symmetry group applied to real crystals and that our model is a better reflection of the real crystal [6].

III. QUASICLASSICAL DYNAMICS AND CHAOS

In the first place, we shall analyze the quasiclassical counterpart of Hamiltonian (1), which is given by

$$H=\frac{1}{2}(P_1^2+P_2^2)+V(\mathbf{Q})+k(\mathbf{Q}\cdot\boldsymbol{\sigma}), \tag{4}$$

where the first term is a kinetic energy for classical vibrational modes with coordinates $\mathbf{Q}=(Q_1,Q_2)$, the second one is the harmonic and/or anharmonic potential, and the third one is the quasiclassical form for the Jahn-Teller interaction where $\boldsymbol{\sigma}$ is Pauli matrices $\sigma=(\sigma_x,\sigma_y,\sigma_z)$. Noting that $\boldsymbol{\sigma}$ space is independent of the real space, we choose σ_x, σ_y, and σ_z corresponding to σ_2, σ_3, and σ_1, respectively. It is convenient to represent the quantum state by using the density matrix $\boldsymbol{\rho}$:

$$\boldsymbol{\rho}=\frac{1}{2}\begin{pmatrix}1+z & x-iy\\ x+iy & 1-z\end{pmatrix}, \tag{5}$$

where $\mathbf{r}=\mathrm{Tr}(\boldsymbol{\rho}\sigma)=(x,y,z)\equiv(\mathbf{r}_\perp,z)$ is a real vector. Using the potential

$$V(\mathbf{Q})=V_0(\mathbf{Q})+V_A(\mathbf{Q}) \tag{6}$$

with V_0 and V_A in Eqs. (2) and (3), the equations of motion derived from Eq. (4) are

$$\frac{d\mathbf{Q}}{dt}=\mathbf{P}, \tag{7a}$$

$$\frac{d\mathbf{P}}{dt}=-\frac{dV(\mathbf{Q})}{d\mathbf{Q}}-k\mathbf{r}_\perp, \tag{7b}$$

$$\frac{d\mathbf{r}}{dt}=k\mathbf{Q}\times\mathbf{r}. \tag{7c}$$

Equation (7c) is nothing but the Schrödinger equation $i\dot{\rho}=[H,\rho]$, from which we find the constant of motion $|\mathbf{r}|=1$. In the study of quasiclassical dynamics, our interest lies in qualitative comparison between the systems with and without the anharmonic term, and therefore we confine ourseleves to the adiabatic limit $dz/dt=0$, that is, $\mathbf{r}=(\mathbf{r}_\perp,z_0)$ with $\mathbf{r}_\perp^2=1-z_0^2$. Further, we find from Eq. (7c)

$$\frac{dz}{dt}\mathbf{e}_z=k\mathbf{Q}\times\mathbf{r}_\perp=0,$$

which is satisfied only when $\mathbf{r}_\perp\|\mathbf{Q}$. Thus the adiabatic limit is equivalent to

$$\mathbf{r}_\perp=\sqrt{1-z_0^2}\,\frac{\mathbf{Q}}{Q}, \tag{8}$$

where $Q=|\mathbf{Q}|$. Using Eq. (8), Eq. (7b) reduces to

$$\frac{d\mathbf{P}}{dt}=-\frac{dV(\mathbf{Q})}{d\mathbf{Q}}-\tilde{k}\frac{\mathbf{Q}}{Q} \tag{9}$$

with the renormalized coupling $\tilde{k}=k\sqrt{1-z_0^2}$. In our adiabatic approximation, we have no interesting fictitious magnetic field induced by the conical intersection in Fig. 1 [17–20], since both $\mathbf{Q}$ and $\mathbf{P}$ here are two dimensional. Further, for our purpose to explore the onset of chaos in a wide parameter range, the adiabatic approximation will be the most effective except when the energy is of the order of $k^2/2\omega^2$. Consequently, the classical equation of motion for

the present model can be expressed only by $\mathbf{Q},\mathbf{P}$ and consists of a set of Eqs. (7a) and (9). This set has the first integral of motion or the total energy

$$E=\frac{\mathbf{P}^2}{2}+V(\mathbf{Q})+\tilde{k}\frac{\mathbf{Q}^2}{Q}. \tag{10}$$

The following analysis depends on the type of the potential $V(\mathbf{Q})$. First, we investigate the system with the harmonic potential only, i.e., $V(\mathbf{Q})=V_0(\mathbf{Q})$. In this case, in addition to the total energy (10), we have another constant of motion, i.e., the orbital angular momentum

$$J_z=(\mathbf{Q}\times\mathbf{P})_z. \tag{11}$$

The number of constants of motion agrees with the degrees of freedom (two). Therefore the system is integrable [9,21,22], showing only regular motions. Then, we investigate the system with the anharmonic potential $V(\mathbf{Q})=V_0(\mathbf{Q})+V_A(\mathbf{Q})$. The trigonal field on the 2D plane (Q_1,Q_2) is invariant only to operations of the cubic group [6]. Owing to this breaking of continuous circular symmetry, the angular momentum J_z in Eq. (11) is not a constant of motion, which makes the system nonintegrable. It should be noted that the lattice system without coupling with the electronic degree of freedom is identical to the Hénon-Heiles system whose dynamical features have been intensively studied in a context of chaos theory [9,23].

The present system has two control parameters, i.e., the coupling constant $\tilde{k}$ between electronic and vibrational degrees of freedom and the nonlinearity parameter b responsible for the trigonal field. However, the simple scaling below lets them merge to a relevant single parameter. Let the coordinates (Q_1,Q_2) be transformed to (q_1,q_2) through $\sqrt{b/\tilde{k}}Q_1=q_1$, $\sqrt{b/\tilde{k}}Q_2=q_2$. The total energy is then written as

$$E=\frac{1}{2}\frac{\tilde{k}}{b}\left(\frac{d\mathbf{q}}{dt}\right)^2+\frac{\omega^2}{2}\frac{\tilde{k}}{b}\mathbf{q}^2+\frac{\tilde{k}^{3/2}}{\sqrt{b}}\left[\frac{1}{2}\sqrt{q_1^2+q_2^2}+\frac{q_1^3}{3}-q_1q_2^2\right]. \tag{12}$$

Next, define the scaled time $\tau=(\tilde{k}b)^{1/4}t$ and the scaled momentum $\mathbf{p}=d\mathbf{q}/d\tau$. Finally, by scaling the energy and the angular frequency as

$$\epsilon=Eb^{1/2}\tilde{k}^{-3/2}, \tag{13a}$$

$$\Omega^2=\omega^2\tilde{k}^{-1/2}b^{-1/2}, \tag{13b}$$

the total energy is expressed as

$$\epsilon=\frac{1}{2}\mathbf{p}^2+\frac{1}{2}\Omega^2\mathbf{q}^2+\frac{1}{2}\sqrt{q_1^2+q_2^2}+\frac{q_1^3}{3}-q_1q_2^2. \tag{14}$$

Eliminating $\tilde{k}$ from Eqs. (13a) and (13b), we find $\epsilon=(\Omega/\omega)^6Eb^2$, which tells that the enhancement of the anharmonic term is equivalent to the increase of the scaled energy ϵ under a fixed value of Ω/ω. In our numerics below, we choose $\Omega/\omega=1$. Figure 2 shows Poincaré surface of sections for energies $\epsilon=0.01$, 0.4, and 0.7. While in Fig. 2(a) we find almost all trajectories to be regular, Fig. 2(b) shows that Kolmogorov-Arnold-Moser (KAM) trajectories begin to collapse and some trajectories become chaotic. Finally, in Fig. 2(c) chaotic trajectories dominate almost all phase space. These results imply that the domain of chaos expands gradually with increasing the scaled energy or the anharmonicity under a fixed value of the scaled angular frequency.

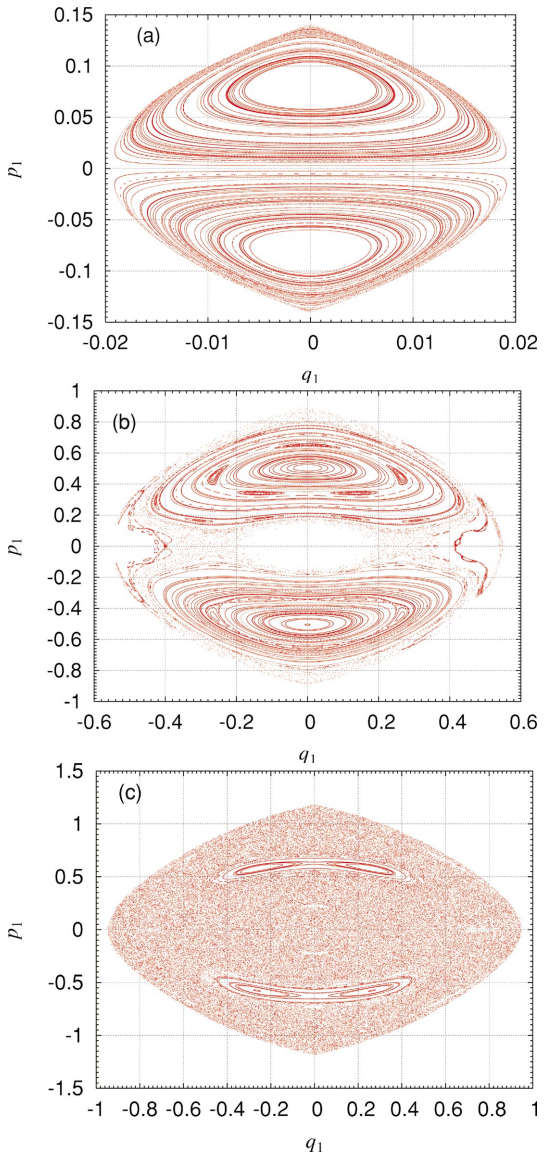

FIG. 2. (Color) Poincaré sections at $p_2=0$. $\Omega/\omega=1$. (a) $\epsilon=0.01$, (b) $\epsilon=0.4$, and (c) $\epsilon=0.7$. The scaling of units is written in the text.

We have also solved Eq. (7) without use of the adiabatic approximation. Then, the degree of freedom becomes three. In case that k and b are less than unity, the relative fraction of chaos in phase space is quite small: We call this behavior "partial chaos." However, if both k and b are as large as 5, the global chaos as seen in Fig. 2(c) appears. In case of $b=0$, we find no indication of irregularity. We shall now proceed to investigate a quantal counterpart of these classical features.

IV. QUANTUM SYSTEMS

In this section we investigate the quantal manifestation of chaos and of regular motions without resorting to the adiabatic limit. The construction of the energy matrix is as follows (see Refs. [11] and [24]): The basis wave function is described as the product of electronic wave functions $u_{\pm}(\mathbf{r})$ and vibrational ones $\phi(\mathbf{Q})$. The former is given in terms of $u(\mathbf{r})$ and $v(\mathbf{r})$ below Eq. (1) as

$$u_{\pm}(\mathbf{r})=\frac{1}{\sqrt{2}}[u(\mathbf{r})\pm iv(\mathbf{r})], \tag{15}$$

while the latter is the eigenstate with the eigenvalue $E_{nm}=n\hbar\omega$ for the 2D harmonic oscillator:

$$\phi_{n,m}(\rho,\theta)=F_{n|m|}(\rho)e^{im\theta}, \tag{16}$$

where $n=1,2,\ldots$ and $m=n-1,n-3,\ldots,-n+1$. $F_{n|m|}(\rho)$ is the confluent hypergeometric function [24]. Thus, the basis wave functions for the present model are given by

$$\Phi^{\pm}_{n,m}=u_{\pm}(\mathbf{r})\phi_{n,m}(\rho,\theta). \tag{17}$$

Corresponding to Eq. (1), the interaction matrix H_{JT} is expressed as

$$H_{\mathrm{JT}}=V_u(\mathbf{r})Q_1+V_v(\mathbf{r})Q_2=\frac{\rho}{\sqrt{2}}[V_{u-}(\mathbf{r})e^{i\theta}-V_{u+}(\mathbf{r})e^{-i\theta}] \tag{18}$$

with the matrix elements of $V_{u\pm}$ given by

$$\langle u_{\pm}|V_{u+}(\mathbf{r})|u_{\pm}\rangle=\langle u_{\pm}|V_{u-}(\mathbf{r})|u_{\pm}\rangle=0,$$

$$\langle u_{\mp}|V_{u\pm}(\mathbf{r})|u_{\pm}\rangle=\mp\sqrt{2}k. \tag{19}$$

As for the lattice-vibration factor $\rho e^{\pm i\theta}$ in Eq. (18), we have nonvanishing matrix elements as

$$\langle\phi_{n,m}|\rho e^{-i\theta}|\phi_{n+1,m+1}\rangle=\langle\phi_{n+1,m+1}|\rho e^{i\theta}|\phi_{n,m}\rangle=\left[\frac{\hbar}{2\omega}(n+m+1)\right]^{1/2},$$

$$\langle\phi_{n,m}|\rho e^{-i\theta}|\phi_{n-1,m+1}\rangle=\langle\phi_{n-1,m+1}|\rho e^{i\theta}|\phi_{n,m}\rangle=\left[\frac{\hbar}{2\omega}(n-m-1)\right]^{1/2}.$$

As a result, the matrix elements for Eq. (18) are

$$\langle\Phi^{+}_{n,m}|H_{\mathrm{JT}}|\Phi^{-}_{n',m'}\rangle=k\langle\phi_{n,m}|\rho e^{i\theta}|\phi_{n',m'}\rangle=k\left\{\frac{\hbar}{2\omega}[n\pm(m-1)]\right\}^{1/2}\delta_{n',n\mp1}\delta_{m',m-1}, \tag{20}$$

$$\langle\Phi^{-}_{n,m}|H_{\mathrm{JT}}|\Phi^{+}_{n',m'}\rangle=k\langle\phi_{n,m}|\rho e^{-i\theta}|\phi_{n',m'}\rangle=k\left\{\frac{\hbar}{2\omega}[n\pm(m+1)]\right\}^{1/2}\delta_{n',n\pm1}\delta_{m',m+1}. \tag{21}$$

If we assign the quantum numbers $j=\pm1$ to $\Phi^{\pm}_{n,m}$, H_{JT} without the anharmonic term connects the states with the same quantum number, $\ell=m-(1/2)j$ $(j=\pm1)$. As discussed by Longuet-Higgins [11], the present matrix decomposes into matrices labeled by quantum number ℓ. For any given value of ℓ, m can take two values $\ell-1/2$ and $\ell+1/2$ corresponding to $j=-1$ and $+1$, respectively. Thus, the pth eigenfunction for a given ℓ is expressed as $\Psi_{p,\ell}$. If we consider the trigonal field (3), levels with $\ell\pm3N$ $(N=1,2,3,\ldots)$ are coupled to levels of ℓ, as discussed in Ref. [11]. The energy matrix is decomposed into only three irreducible presentations A_g, B_g, and E_g. By the exact diagonalization of each submatrix for the Hamiltonian including H_{JT}, we can get eigenvalues and eigenvectors. The result depends on two parameters, the coupling constant k and the strength of the trigonal field b.

Here, we concentrate on the nearest-neighbor level-spacing distribution $P(s)$, which plays a prominent role in the quantum description of classically chaotic quantum systems. The random matrix theory presents a natural framework for describing fluctuation properties of spectra of quantum systems, whose corresponding classical model exhibits chaotic behaviors. In fact the correlations in Gaussian ensembles of random matrices are found to match very closely the empirical correlations among energy levels in classically chaotic systems. If the phase space is totally chaotic, the distribution of level spacings is Wigner-like [Guassian orthogonal ensemble (GOE)],

$$P_w(s)=\frac{\pi}{2}s\,\exp\left(-\frac{\pi}{4}s^2\right).$$

By contrast, in classically regular quantum systems the levels are independent of each other, and therefore the spacings obey Poisson distribution,

$$P_p(s)=\exp(-s).$$

Considering these standard criteria, we present the level-spacing distribution for the Hamiltonian (1) in the following.

First, we consider the system without trigonal field ($b=0$). For the manifold of $\ell=1/2\pm3m$ $(m=0,1,2\ldots,)$, Fig. 3(a) shows level-spacing distribution characterized by the Poisson distribution, which tells that this system is regular in the classical dynamics [25]. Figure 3(b) shows integrated values of histograms in shown Fig. 3(a), which well fits the function $1-e^{-s}$.

Then we reveal the role of trigonal field. Figure 4 shows the dependence of eigenvalues on the parameter b, where a multitude of avoid crossings can be found.

Figure 5(a) shows a level-spacing distribution in the case of $b=5$. It should be noted that the distribution perfectly agrees with the Wigner one with $P(s)\rightarrow s$ as $s\rightarrow0$. In Fig.

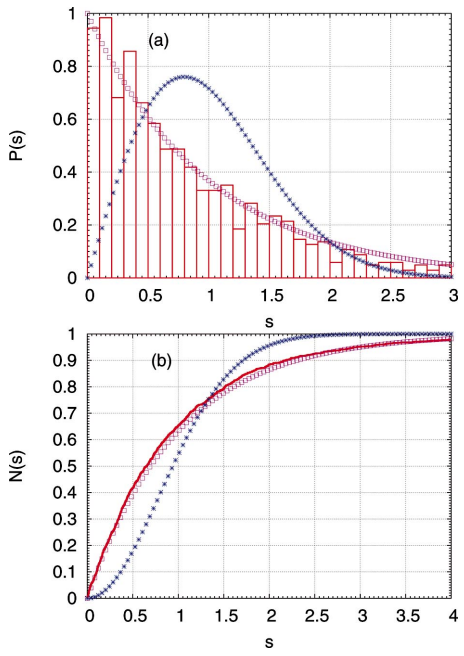

FIG. 3. (Color) (a) Histograms of level-spacing distribution for $k=4,b=0$ (without trigonal field). Curves of Poisson distribution and GOE are also drawn by open rectangles and crosses, respectively. (b) Integrated level-spacing distribution with the use of data in (a).

5(b) we show the corresponding integrated level-spacing distribution, which also well fits the Wigner one (GOE). We would like to point out the following fact: In the corresponding classical system with $k=4$ and $b=5$ without the use of the adiabatic approximation, the almost whole regions in the phase space exhibit stochastic behavior. However, the system under consideration is generic: the phase space of the underlying classical dynamics consists of both regular KAM tori and chaos. In fact, for the relatively small value of b (e.g., $0<b\lesssim 1$), we get the Brody distribution which interpolates the Poisson and the Wigner ones. In the semiclassically asymptotic limit of sufficiently small effective Planck constant, one would expect the Berry-Robnik distribution [26–28] that allows us to estimate the relative measure of the chaotic part in the classical phase space. The Brody distribution is more effective in the present analysis, however, because we are concerned with the quantal rather than the semiclassical regime.

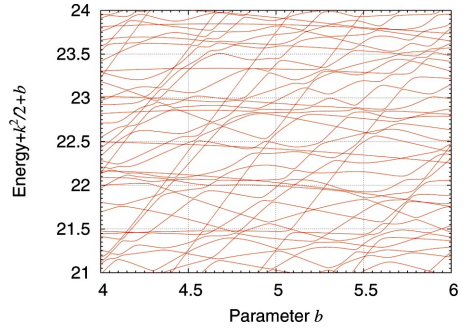

FIG. 4. (Color) Dependence of eigenvalues ($\sim p=120$) on anharmonic parameter b. The unit of energy is $\hbar\omega$.

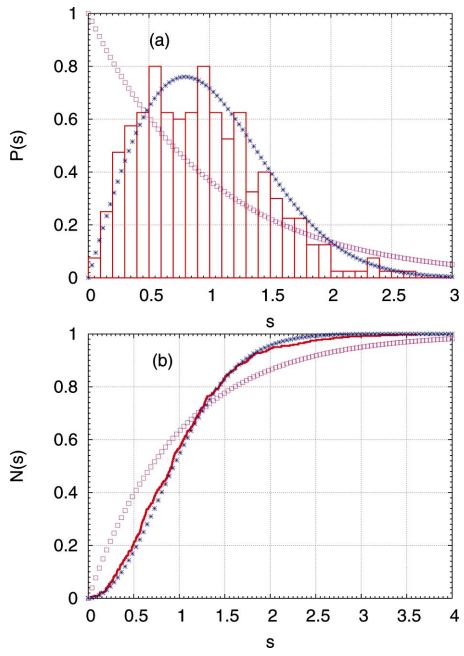

FIG. 5. (Color) (a) Histograms of level-spacing distribution. (b) Integrated level-spacing distribution for $k=4,b=5$ (with trigonal field). Curves of Poisson distribution and Wigner distribution are also drawn by open rectangles and crosses, respectively.

In addition, we investigate the wave-function statistics. We focus on the probability density to find the first basis state $[\Phi^{-}\equiv u_{-}(\mathbf{r})\phi_{1,0}(\rho,\theta)]$ populated in each of the ensemble of eigenstates. To be explicit, we choose the scaled probability density $x\equiv|a_{1p}|^2/\overline{a^2}$ as a stochastic variable, where a_{1p} is the first coefficient to appear later [in Eq. (23)] and $\overline{a^2}$ stands for the average of $|a_{1p}|^2$ over the ensemble of eigenstates.

Figure 6 shows a wave-function statistics for the scaled probability density in the case of $k=4$, $b=5$. We find that the histogram almost agrees with Porter-Thomas distribution

$$P_{\text{Porter-Thomas}}(x)=\frac{1}{\sqrt{2\pi x}}\exp(-x/2),$$

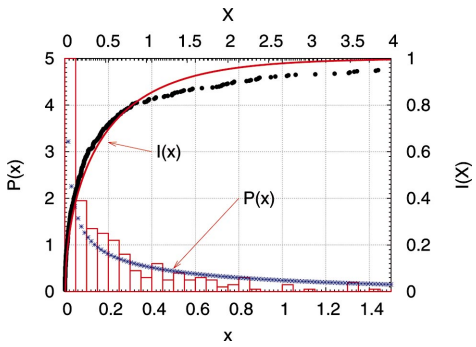

FIG. 6. (Color) Histograms of the wave-function statistics for density distribution for the case of $k=4$, $b=5$ with trigonal field; integrated density distribution is shown by black circles. Curves of Porter-Thomas distribution $P(x)$ and integrated Porter-Thomas one $I(X)$ are also drawn by crosses and thin line, respectively.

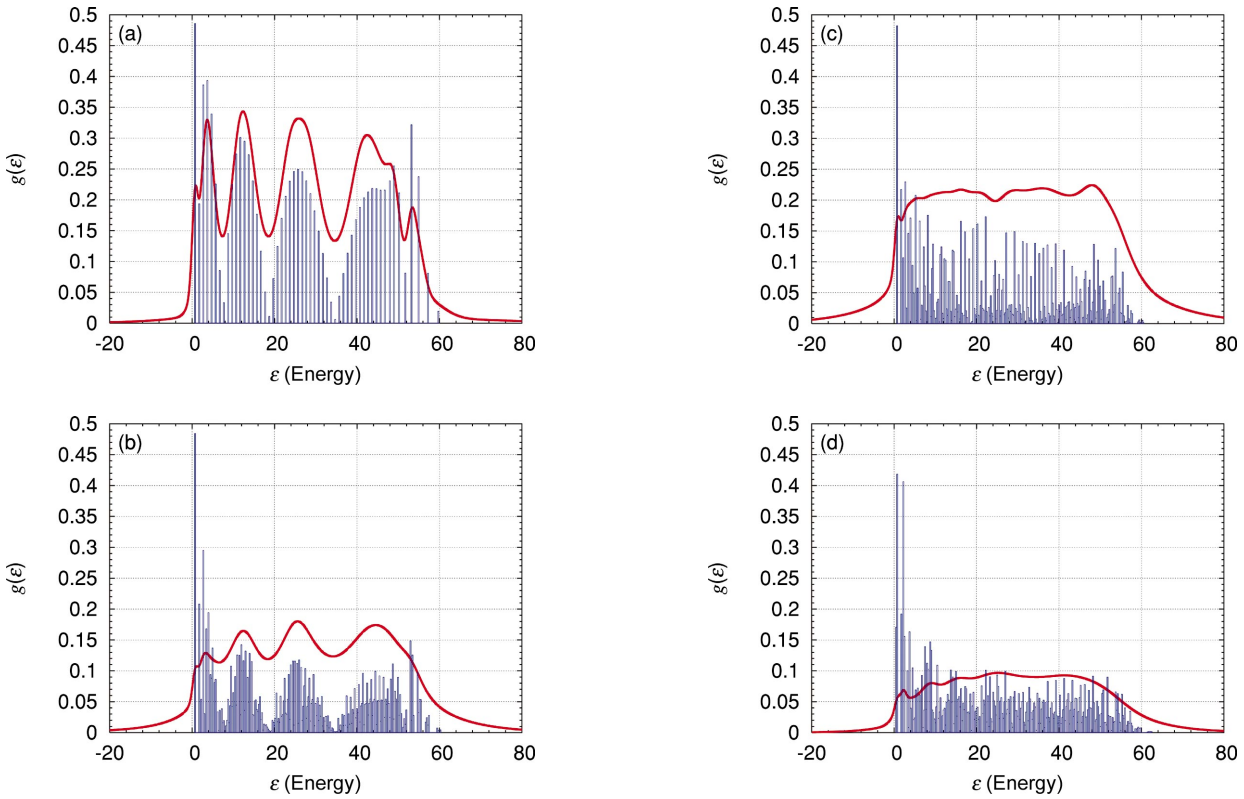

FIG. 7. (Color) g factor $g(\varepsilon)d\varepsilon$ ($\varepsilon=0.25$) for the electronic orbital angular momentum. $\ell=1/2$ and $k=0.707$. (a), (b), (c), and (d) correspond to $b=0$, 0.2, 0.3, and 1.41, respectively. The unit of energy is $\hbar\omega$. Envelop functions composed for Gaussian distribution types are also depicted.

whose significance was realized at ''the dawn of random matrix theory.''

While most of the studies on quantum chaos have been limited to the analysis of level-spacing distributions, of wave-functions scars and Thomas-Porter distribution, we shall here embark upon the investigation of experimentally accessible new indicators. We pay attention to magnetism in the dynamical Jahn-Teller system. In particular, we discuss the magnetic g factor in the following section [29].

V. ELECTRONIC ORBITAL ANGULAR MOMENTUM

The essential features of the Jahn-Teller coupled systems are caused by the interaction between the nuclear motions and the electrons in non-Kramers doublets for multiplets of d levels. In particular, the quenching of the electronic orbital angular momentum—the so-called magnetic g factor—in those doublets is the fundamental subject in magnetism of transition-metal ionic compounds. As well known, the static Jahn-Teller effect removes the ground state degeneracy of electronic states. This effect leads to the complete disappearance of the orbital angular momentum, leaving only spin degree of freedom. On the other hand the dynamic Jahn-Teller systems for the relatively weak coupling have a possibility of the nonvanishing orbital angular momentum in non-Kramers doublets because of the continuous distortion of lattices. In fact, in the absence of a trigonal field the $E_g \otimes e_g$ system has the freedom of the continuous distortion of lattices along the continuous minima of the adiabatic ''Mexican hat'' potential.

Washimiya [29] payed attention to the dependence of expectation value of this orbital angular momentum $\langle L_z\rangle$ in the excited levels $\Psi_{p,\ell}$ derived in Sec. IV. He pointed out the oscillatory behavior of $\langle L_z\rangle$ with increasing energy levels. The nonvanishing values $\langle L_z\rangle$ are given as

$$\begin{aligned}\langle L_z\rangle_p &= \langle \Psi_{p,\ell=1/2}|L_z|\Psi_{p,\ell=1/2}\rangle \\ &= \left[\sum_{n=1}^{\infty}(-1)^n a_{n,p}^2\right]\Xi, p \\ &= 1,2,3,\ldots \end{aligned} \tag{22}$$

for the vibronic state of $\ell=1/2$. Here, $a_{n,p}$'s are the coefficients of the harmonic oscillator functions. As already mentioned, the vibronic wave function is given by

$$\begin{aligned}\Psi_{p,\ell} = {} & a_{1p}u_-(\mathbf{r})\phi_{1,0}(\rho,\theta) + a_{2p}u_+(\mathbf{r})\phi_{2,1}(\rho,\theta) \\ & + a_{3p}u_-(\mathbf{r})\phi_{3,0}(\rho,\theta) + a_{4p}u_+\phi_{4,1}(\rho,\theta) + \cdots . \end{aligned} \tag{23}$$

In Eq. (22), Ξ represents the elements in the principal diagonal of the matrix ($\Xi=\langle u_+|L_z|u_+\rangle=-\langle u_-|L_z|u_-\rangle$). In short, the differences of $|a_{n,p}|^2$ between even- and odd- numbers of n in the eigenfunction labeled by p play an essential role. As p increases, the oscillatory behavior of the angular

momentum is found. The periods of this oscillation are far long in comparison with the variation by odd and even numbers for the small coupling k. With increasing k, the absolute value of the angular momentum decreases. The origin of this oscillation has not been clarified up to now, though Washimiya's finding is essential for understanding properties of this vibronic systems.

In what follows, we show a more detailed calculation of this oscillatory behavior. Furthermore, the effect of the trigonal field is discussed in consideration that this field destroys the continuous circular symmetry and that the angular momentum ℓ is not a good quantum number. Under this condition, we introduce the density of g factor $g(\varepsilon)d\varepsilon$ for the electronic orbital angular momentum in the energy range between ε and $\varepsilon+d\varepsilon$ as

$$g(\varepsilon)d\varepsilon=\sum_{p}{}' \left|\sum_{n=1}^{\infty}(-1)^n a^2_{\ell=1/2,n,p}\right| d\varepsilon. \qquad (24)$$

Here, the summation of p is taken over the corresponding energy range. It should be noted that levels for $\ell'=1/2 \pm 3N(N=1,2,\ldots)$ are mixed with the levels for $\ell=1/2$ in the presence of the trigonal field.

We show calculated results of $g(\varepsilon)$ at $k=0.707$ in Fig. 7. In Fig. 7(a), the regular oscillatory behavior of $g(\varepsilon)$ for $b=0$ as a function of level p, which was reported by Washimiya [29] three decades ago, is reproduced. In addition to histograms for $g(\varepsilon)$, we also show the envelop functions constructed by Gaussian coarse graining of each peak. Figures 7(b), 7(c), and 7(d) show the ε dependence of $g(\varepsilon)$ in the presence of trigonal field with $b=0.2$, 0.3, and 1.41, respectively. Here, we can find the suppression of regular oscillation with increasing b.

The emergence of irregular oscillation and the suppression of the g factor with increasing b reflects the underlying chaotic behavior in Sec. III. We find the important fact: while the level statistics can reach the Wigner distribution for a sufficiently large value of b, the suppression of the regular oscillation of the g factor easily occurs for a relatively small value of b. In fact the values of $b=1.41$, $k=0.707$ ($\Omega/\omega=1$, $kb=1$) in Fig. 7(d) are much less than the values of $b=5$, $k=4$ that guarantee the Wigner distribution in the case without the adiabatic approximation. As a result, the irregular oscillation of the g factor is a precursor of quantum chaos, namely, the suppression of its regular oscillation occurs even when the classical phase space accommodates a partial chaos.

VI. SUMMARY AND DISCUSSIONS

We have examined the Jahn-Teller $E_g\otimes e_g$ system from a viewpoint of classical chaos and its quantization. Both the systems A without a trigonal anharmonic term and B with it are investigated.

The classical phase space is strictly regular for the system A and nonintegrable and chaotic for the system B. In general, the system B is mixture of regular KAM tori and chaos. The relative fraction of chaos in the phase space increases as the energy or the strength of the anharmonicity is increased. In the adiabatic approximation, the full chaos can occur easily because of enhancement of nonlinear effects due to the strong constraint. Without such an approximation, we can find the full chaos for relatively large values of k and b, and obtain only the partial chaos, if we adopt small values to k and b.

For the corresponding quantum systems, the level-spacing distributions are shown to be of Poisson- and Wigner-type for the systems A and B, respectively. We find that the Wigner distribution is available as well by adopting the relatively large values of k and b. On the other hand, the dependence of g factors on energy ε is a quite sensitive indicator of the symptom of chaos in comparison with the level-spacing distribution. In the system A the g factor shows regular oscillation with respect to excitation energy. By contrast, in the system B it shows a quenched irregular oscillation for the relatively small values of k and b. Therefore, we propose the magnetic g factor as a new precursor of quantum chaos, superior to the level-spacing distribution. We hope that these predictions will be verified in future such as in the experiment of magnetic circular dichromism.

It will be quite important that the precursor of chaos shows up in the observable orbital angular momentum in the dynamical Jahn-Teller systems for transition-metal ionic-compounds. There are other interesting themes in this system, such as an effect of the chaos on a spectral feature of phonon side bands, which will also be examined in due course.

[1] H-J. Stöckmann, *Quantum Chaos: An Introduction* (Cambridge University Press, Cambridge, 1999).

[2] F. Haake, *Quantum Signatures of Chaos* (Springer, Berlin, 1991).

[3] R. Blümel and W. P. Reinhardt, *Chaos in Atomic Physics* (Cambridge University Press, Cambridge, 1997).

[4] K. Nakamura, *Quantum versus Chaos* (Kluwer Academic Publishers, Dordrecht, 1997).

[5] K. F. Berggren and S. Åberg, *Quantum Chaos Y2K: Proceedings of the Nobel Symposium* (Royal Swedish Academy of Science/ World Scientific, Singapore, 2001).

[6] S. Sugano, Y. Tanabe, and H. Kamimura, *Multiplets of Transition-Metal Ions in Crystals* (Academic Press, New York, 1970).

[7] M. V. Berry, Proc. R. Soc. London **392**, 45 (1984).

[8] A. Shapere and F. Wilczek, *Geometric Phase in Physics* (World Scientific, Singapore, 1989).

[9] A. J. Lichtenberg and M. A. Lieberman, *Regular and Chaotic Dynamics* (Springer-Verlag, Berlin, 1990).

[10] H. Koizumi and I.B. Bersuker, Phys. Rev. Lett. **83**, 3009 (1999).

[11] H.C. Longuet-Higgins, U. Öpik, and M. H. L. Pryce, Proc. R. Soc. London, Ser. A **244**, 1 (1958).

[12] C. A. Mead, Rev. Mod. Phys. **64**, 51 (1992).

[13] M. C. M. O'Brien, Proc. R. Soc. London, Ser. A **281**, 323 (1964).
[14] M. L. Mehta, *Random Matrices* (Academic Press, New York, 1967).
[15] O. Bohigas, M. J. Giannoni, and C. Schmit, Phys. Rev. Lett. **52**, 1 (1984).
[16] T. Takami and H. Hasegawa, Phys. Rev. Lett. **68**, 419 (1992).
[17] A. Bulgac, Chaos Solitons Fractals **5**, 1051 (1995).
[18] A. Bulgac, Phys. Rev. A **37**, 4084 (1988).
[19] A. Bulgac and D. Kusnezov, Ann. Phys. (N.Y.) **199**, 187 (1990).
[20] D. Kusnezov, Phys. Rev. Lett. **72**, 1994 (1994).
[21] K. Nakamura, *Quantum Chaos—A New Paradigm of NonLinear Dynamics* (Cambridge University Press, Cambridge, 1993).
[22] V. I. Arnold, *Mathematical Methods of Classical Mechanics* (Nauka, Moscow, 1974).
[23] M. Brack and R. K. Bhaduri, *Semiclassical Physics* (Addison-Wesley, Reading, MA, 1997).
[24] L. Pauling and E. B. Wilson, *Introduction to Quantum Mechanics* (McGraw-Hill, New York, 1935).
[25] M. V. Berry and M. Tabor, Proc. R. Soc. London, Ser. A **356**, 375 (1977).
[26] M. Berry and M. Robnik, J. Phys. A **17**, 2413 (1984).
[27] M. Robnik, Nonlinear Phenomena in Complex Systems (Minsk) **1**, 1 (1998).
[28] T. Prosen and M. Robnik, J. Phys. A **27**, 8059 (1994).
[29] S. Washimiya, Phys. Rev. Lett. **28**, 556 (1972).